Core-Shell Nanocapsules Stabilized by Single-Component Polymer and Nanoparticles for Magneto-Chemotherapy/ Hyperthermia with Multiple Drugs

*Shang-Hsiu Hu, Bang-Jie Liao, Chin-Sheng Chiang, Po-Jung Chen, I-Wei Chen, and San-Yuan Chen**

Chemotherapy is well known to have several severe and common problems such as toxic side effects and drug resistance. One approach that can mitigate the side effect is targeted delivery using nanoparticles that conceal the drug until they reach the tumor. However, to timely trigger drug release once at the tumor site is not straightforward, and its execution may greatly influence the outcome of chemotherapy. Meanwhile, one approach that can reduce drug resistance is to use multiple drugs to eradicate all malignant cells at once.[1–6] However, it is rather difficult to design carriers that can conceal drugs of drastically different physical chemistry, such as hydrophobic paclitaxel (PTX) and hydrophilic doxorubicin (DOXO). (Both are potent chemotherapy drugs, made even more effective when used together.[7–9]) Moreover, it is extremely difficult to achieve timely release of multiple drugs from such carriers. Yet reaching high concentrations of all drugs at the same time is often required to successfully implement the multi-drug strategy. Resolving these difficulties will have a significant impact on cancer therapy and patient wellbeing.

These difficulties are fundamentally related to materials issues and challenges on the nanoscale. For example, although most multi-cargo nano systems (micelles, liposomes, and mesoporous silica nanoparticles) can conceal their hydrophobic cargo within, the hydrophilic cargo (including siRNA and gene) is typically left tethered to or adsorbed onto the outer surfaces of the carriers.[1,2,5,6] Therefore, unintended side effects caused by the hydrophilic cargo may be unavoidable, and the release of the hydrophobic cargo most likely will lag. Another example is the water-in-oil-in-water (W/O/W) nanoparticle which is a popular construct for co-delivering multiple drugs.[10–13] It has a small water-like core within an oil-like shell that is surrounded by an amphipathic surfactant.[14–16] But such particles are typically produced by the two-step double emulsifying method (first forming a water-in-oil (W/O) emulsion, then adding water to form a W/O/W emulsion), which with few exceptions[14] cannot yield a size small enough (say <200 nm) for in vivo circulation. Furthermore, there is commonly a need for using multiple surfactants during the two-step emulsifying procedure, which inevitably adds chemical/processing complexity and may raise potential concerns for the in vivo use of the product.[14,15] Lastly, the kinetics of drug release from the core most likely will lag behind that from the shell, thus compromising the goal of simultaneous rapid release often essential for the multi-drug strategy.

Here we propose a new nanocarrier platform for multiple-drug co-delivery and on-demand release, based on a new family of W/O/W core-shell nanocapsules made from the self assembly of a one-component polymer and magnetic nanoparticles. In this approach, the polymer constitutes the shell but also serves as the surfactants, and the magnetic nanoparticles stabilize the shell but also serve as the sensor/actuator that triggers drug release. We achieved these goals by carefully screening biocompatible polymers (in particular poly(vinyl alcohol) (PVA)) for their hydrophobic/hydrophilic properties, and by designing magnetic nanoparticles (in particular iron oxide (IO)) that can reside in the polymer shell during self-assembly. The designed core-shell naocapsules carry hydrophilic DOXO in the core and hydrophobic PTX in the shell, both drugs showing little release until the release is triggered by an external magnetic field. Since magnetic induction of IO also gives rise to local heating, both magneto-chemotherapy and magneto-hyperthermia contribute to cell kill and tumor treatment, adding to the already synergetic effect of PTX and DOXO. Enhanced delivery is further achieved by conjugating a tumor-targeting peptide to the nanocapsules.

As mentioned above, the so-called core-shell, double-emulsion capsules (DEC) are usually prepared by a two-step emulsifying process, with surfactants often added in one or both steps to stabilize emulsions. Here we aim to obtain the same construct from a surfactant-free one-step emulsifying process, which (a) includes IO nanoparticles as DEC stabilizers, forming DEC-IO, and (b) uses PVA as both the shell constituent and the surfactant. As schematically shown in the upper panel of **Figure 1**a, when a water phase (de-ionized water) with dissolved PVA of an intermediate molecular weight (MW) (e.g., PVA-16k having MW = 16 000 g/mol) is mixed with an oil phase (chloroform) containing hydrophobic IO nanoparticles (5 nm) synthesized from an oleic acid process, an emulsion containing W/O/W DEC (e.g., DEC-16k-IO) forms with the IO localized in the PVA (e.g., PVA-16k) shell of the DEC-IO. The key characteristics of the DEC-IO synthesized with PVA-16k, PVA-47k and

Dr. S.-H. Hu, B.-J. Liao, C.-S. Chiang, P.-J. Chen, Prof. S.-Y. Chen
Department of Materials Science and Engineering
National Chiao Tung University
Hsinchu 300, Taiwan
E-mail: sanyuanchen@mail.nctu.edu.tw
Prof. I.-W. Chen
Department of Materials Science and Engineering
University of Pennsylvania
Philadelphia, PA 19104-6272, USA

DOI: 10.1002/adma.201201251

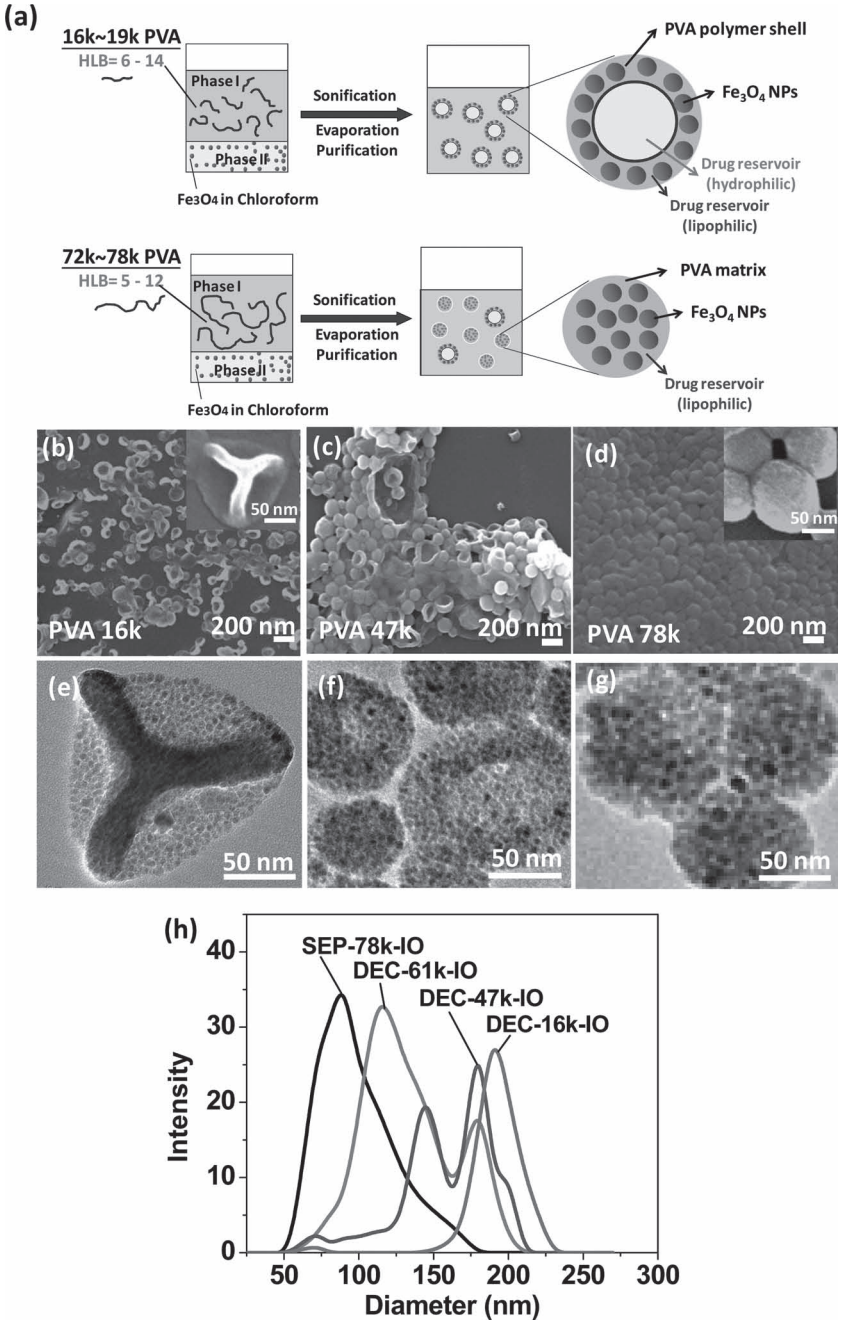

Figure 1. (a) Schematic of one-step emulsion synthesis incorporating IO nanoparticles and single-component polymer PVA. PVA with a MW 16 000 and 19 000 g/mol gives double emulsion capsules (DEC), PVA with a MW of 72 000 and 78 000 g/mol gives single emulsion particles (SEP), PVA with a MW of 23 000 to 67 000 g/mol gives mixtures of both types. SEM and corresponding TEM images of dried DEC-IO and SEP-IO are shown in (b,e) for PVA-16k, (c,f) for PVA-47k, and (d,g) for PVA-78k. (h) Dynamic light scattering data of IO-PVA emulsions of the above compositions (PVA-16k, PVA-61k, and PVA-78k) and of PVA-47k confirming SEP being smaller than DEC.

PVA-61k and their ability to incorporate hydrophilic (DOXO) and hydrophobic (PTX) drugs are summarized in Table S1 (see Supporting Information). To succeed in the above process, both the MW of PVA and the inclusion of IO are crucial. This is elaborated below.

Concerning MW, we found a lower MW PVA (e.g., PVA-10k) favored a W/O emulsion, a higher MW PVA (e.g., PVA-78k) favored an O/W emulsion (the lower panel of Figure 1a) which will be referred to as single-emulsion particle (SEP), only the intermediate MW PVA favored the W/O/W DEC. To determine these MW ranges, screening tests were first conducted by measuring the hydrophilic-lipophilic balance (HLB) value of PVA, which decreases with the MW as described in Figure S1 (see Supporting Information). To ascertain DEC/SEP morphologies, dried W/O/W and O/W emulsion samples (after first oil-chloroform evaporation then water evaporation, under vacuum) were examined by SEM (Figure 1b-d) and TEM (Figure 1e–g). As expected, the O/W SEP made of PVA-78k (Figure 1d,g) are solid spheres of PVA-IO composite. Some spheres are also seen in Figure 1c,f; they tend to be smaller than the other nanoparticles in this PVA-47k formulation. However, many nanoparticles (about 40%) in these latter figures are not spherical, instead, they are concave and have a "bowl-like" appearance. (In the TEM image, Figure 1f, this morphology gives a brighter contrast in the center because of less material scattering of electron beam.) In the PVA-16k formulation where only W/O/W DEC is expected, few solid sphere SEP (6% in Figure 1b) were found. The remaining DEC nanoparticles are mostly hemispherical "bowls", but some have a buckled appearance showing one or more ridges on the back of the "bowls". One such morphology having a set of triangularly branched ridges is highlighted in the inset of Figure 1b, with its TEM image displayed in Figure 1e.

These DEC configurations may be understood using the analogy of a balloon: a wet DEC is like a gas-filled balloon; after drying it collapses just like a deflated balloon. Since the "sac" of DEC-IO is relatively thick and is reinforced by IO nanoparticles, it is relatively rigid capable of supporting a bowl shape or a buckled bowl shape, unlike the "sac" of a collapsed balloon which is cloth-like and flexible. The size of the DEC is evidently larger than that of SEP according to the SEM and TEM images. This is also verified by light scattering measurements of particle size shown in Figure 1h: DEC-16k-IO being larger than SEP-78-IO. The nanocapsules made from PVA of an intermediate MW, DEC-47k-IO and DEC-61k-IO, have a mixed morphology, which is reflected in their bimodal size distributions in Figure 1h. Importantly, this size difference allows the centrifugal separation of DEC and SEP, see the Experimental Section in the Supporting Information, which provided DEC-IO made of PVA of different

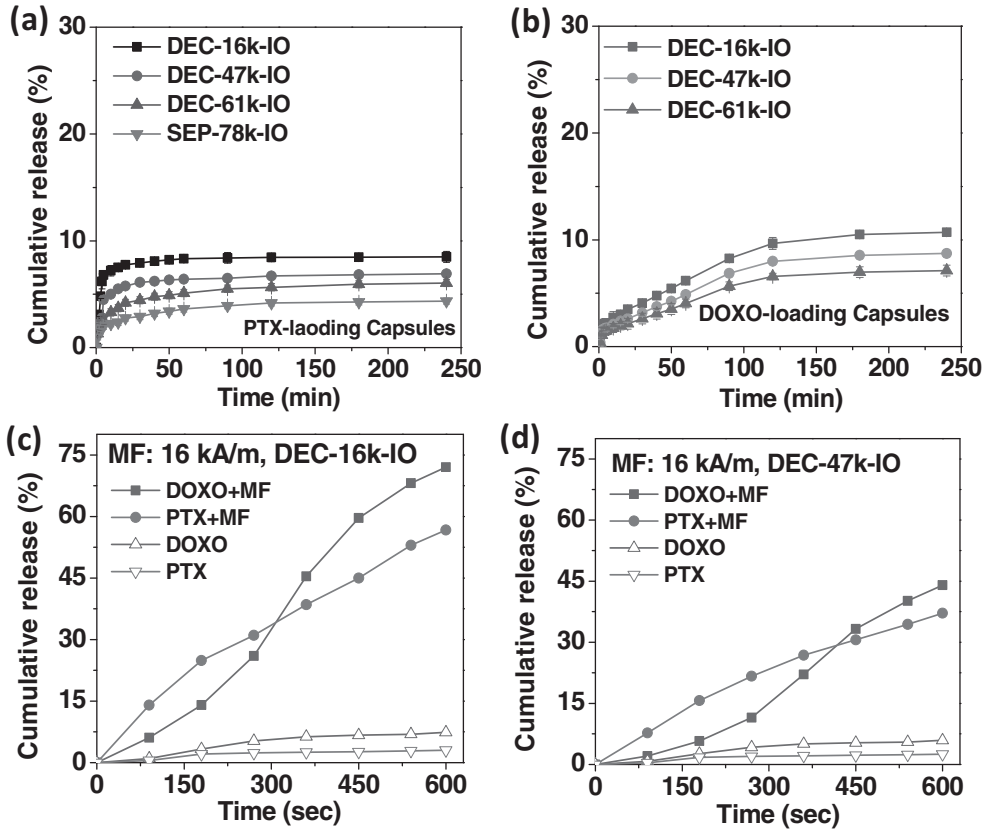

Figure 2. Cumulative drug release of (a) PTX and (b) DOXO from DEC-IO made of PVA of various MW. Accelerating effect of magnetic induction field (MF = 16 kA/m at 50 kHz) on drug release profiles of DOXO and PTX from (c) DEC-16k-IO and (d) DEC-47k-IO is apparent by comparing data with and without MF.

MW used for all subsequent experiments. We also found that the sizes of (wet) emulsion solutions measured by light scattering are only slightly larger than the sizes of the dried particles measured by SEM (Table S1), i.e., there is relatively little shrinkage during drying which is again indicative of the relative rigidity of the IO-reinforced PVA. The size of DEC only modestly decreases with the MW, ranging from 150–160 nm for DEC-16k-IO to 120–130 nm for DEC-67k-IO.

Concerning IO, we note that although PVA is often used as a surfactant to stabilize the outer surface of a W/O/W emulsion that contains an oily shell made of another polymer (e.g., poly[lactic-*co*-glycolic acid] or poly[e-caprolactone]),[17–19] it by itself cannot form a W/O/W emulsion without the assistance of IO. Indeed, we found PVA of a higher MW did form an O/W emulsion, but PVA of a lower MW (after mixing with water and chloroform) did not yield any dry particle/capsule; instead, during drying it simply precipitated into polymeric crystals or thin films. Only when IO was added to the oil phase was it possible to form stable W/O/W DEC with a PVA-IO composite shell. This observation is reminiscent of liquid-liquid interface stabilization by colloidal particles, which is the basis of the so-called (Pickering) solid-stabilized emulsion process.[20–22] Therefore, the combined use of PVA of an intermediate MW (16k–61k) and IO as stabilizing nanoparticles had made possible the discovery of PVA-based DEC for the first time, which we succeeded in forming in a single emulsifying step. We will next load these robust DEC with both hydrophobic (PTX, in the shell) and hydrophilic (DOXO, in the core) cargo, and use the IO in the shell as the magnetic sensor and actuator for triggering cargo unloading on demand. Referring to the phase characterization, magnetization, magnetic relaxation and stability of these DEC (see Figure S2, Supporting Information), we note that they are additionally capable of being excellent contrast agents for MR imaging, which is outside the scope of the present study.

Hydrophobic PTX and hydrophilic DOXO were incorporated into W/O/W DEC-IO, separately (forming DEC-IO-PTX and DEC-IO-DOXO) and in combination (forming DEC-IO-PD). Table S1 (see Supporting Information) lists the encapsulation efficiency (EE%), defined as 100×(amount of drug retained in DEC)/(amount of drug used in preparing emulsion), which exceeds 90% for PTX. For DOXO, the EE% is lower. This could be due to outward DOXO diffusion, through the PVA shell, during emulsification. This scenario is supported by the data of cumulative DOXO release during "storage" in **Figure 2**b, showing a linear release profile which does not slow down until after 2 h. In contrast, PTX has a step release at "zero time" followed by rapid exhaustion (Figure 2a). The difference between DOXO and PTX reflects the different physical property of the two molecules: unlike hydrophilic DOXO, hydrophobic PTX has little driving force for dissolution in the water outside, so it suffers from little release except for the step release at "zero time" which may be attributed to the desorption of the residual PTX left on the DEC surfaces. (PTX having very low solubility in water may have precipitated

onto the DEC surface during emulsion drying.) The systematic effect of MW (from 16 k to 78 k) of PVA on DOXO EE% and release in Figure 2a,b is also consistent with the above interpretation: polymers having a lower MW tend to have a higher permeability due to higher chain flexibility and mobility.

We further studied drug release under the influence of a high-frequency (50 kHz) magnetic field (MF) at various intensities from 4 to 16 kA/m. Two sets of data, for DEC-16k-IO-PD and DEC-47k-IO-PD under 16 kA/m, are shown in Figure 2c,d to demonstrate the following key features. (a) The release rate under MF is much faster than that without MF, as evident from the higher cumulative amount in Figure 2c,d compared to that in Figure 2a,b. (b) The release rate is slower when PVA-47k is used than when PVA-16k is used, which can again be understood in terms of chain flexibility and mobility of PVA. (c) Although the initial release of DOXO is slower than that of PTX, it becomes faster after 3 min causing a crossover of the two cumulative release curves at about 5 min. Since MF is known to cause local heating, and such heating is mediated through the induced magnetization of IO, this observation may indicate that the temperature rise of the PVA-IO shell is initially much larger than that of the surrounding, causing an initially faster release of PTX which resides in the same shell. Later, when the temperature rise spreads througout the core-shell, a faster release of DOXO, further aided by its affinity to water, is realized. (d) After the MF is turned off, the release rate promptly decreases even though the cumulative amount is well below 100% (see Figure S3 in Supporting Information). This suggests that MF does not cause a complete destruction of the DEC, or else all DOXO in the water-phase core should have all been released. Note that our previous studies of DEC without IO in the shell did witness physical rupture and complete destruction of the polymeric shell under similar MF conditions.[23,24] Thus, the DEC-IO is apparently more robust because of the IO reinforcement. (Direct TEM evidence showing intact DEC-IO surviving MF is provided in Figure S4 in Supporting Information.) Additional data for lower MF intensities (8 kA/m and 4 kA/m) are shown in Figure S5 (see Supporting Information) which again manifest the same features but at a lower overall rate that monotonically decreases with decreasing MF intensity. In addition, the data in Figure S6 (see Supporting Information) demonstrate that the PTX/DOXO release profiles of DECs containing only PTX (e.g., DEC-16k-IO-PTX) or only DOXO (e.g., DEC-16k-IO-DOXO) are no different from those of DEC containing both drugs (e.g., DEC-16k-IO-PD), under both MF-free condition and MF condition. Therefore, by placing PTX and DOXO in physically separate compartments in the DEC-IO, we have prevented any drug interaction/interference in their release profiles.

Since MF does induce intense local heating at the nanocapsules as shown in Figure S7a (see Supporting Information), whether it causes damage to the drug molecules or not is an important issue. In Figure S8 (see Supporting Information), we have provided spectroscopic and cell viability data to show that the drugs after MF treatment are still active. Therefore, MF damage is not a concern for these drugs under the test conditions used in this study. These results suggest that it is now feasible to use a remote MF to precisely trigger and control rapid drug release from physically robust DEC-IO carriers.

In vitro cell viability after DEC treatment was determined using HeLa (a human cervical carcinoma cell line) and MCF-7 (a human breast carcinoma cell line) cells incubated with various DEC-16k-IO with and without drugs. First, at a dosage of up to 2 mg/mL DEC for 24 h we demonstrated that drug-free DEC-16-IO was not toxic (cell viability about 90 ± 15%) to cells. (see Figure S8 in Supporting Information). Using DEC labeled with red quantum dots (these hydrophobic nanoparticles also residing in the PVA shell) which emit fluorescence at 600 nm, we further verified that DEC was not taken up by the cells after 8 h; instead, some DEC accumulated at the cell surface. (see Figure S9 in Supporting Information). This is consistent with the IC_{50} (the drug concentration causing 50% cell viability) data of the DOXO/PTX dosage (Table S2 in Supporting Information): encapsulated drug has a much higher IC_{50} than free drug.

To achieve targeted delivery, we conjugated IVO24, a peptide which targets cells of lung, breast, prostate, liver and oral cancer xenografts but not normal tissues, to the surface of DEC using EDC linkers. Again using quantum dot labeling, we verified that DEC conjugated with IVO24 targeted the surfaces of both HeLa and MCF-7 cells after 2 h, and it was internalized after 8 h accumulating in the cytoplasm regions. (see Figure S10 in Supporting Information, which also includes flow cytometry data supporting the same conclusion.) As expected, we found targeting drastically lowered the IC_{50} of the drug carried by DEC, especially when both PTX and DOXO are carried in the same DEC. (See Table S2 in Supporting Information.) To further illustrate the above effects along with the magnetic effect, cytotoxicity experiments at a dosage of up to 6 μg/mL DEC for 24 h. were next conducted using both IVO24-conjugated drug-containing DEC (IVO24-DEC-16k-IO-PTX, IVO24-DEC-16k-IO-DOXO, and IVO24-DEC-16k-IO-PD) and their IVO24-free counterparts, as described below.

The data are plotted in **Figure 3** in seven groups, for both cell lines. (For brevity, MW (16 k) and IO are omitted in the

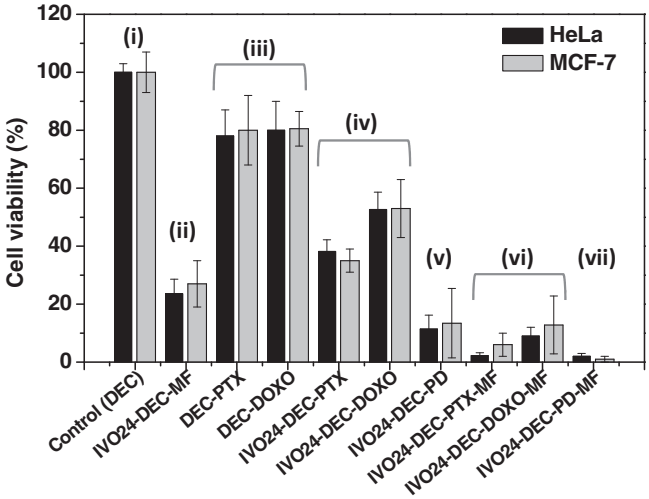

Figure 3. Cell viability after incubating cells (HeLa and MCF-7) for 24 h with DEC of the following types: (i) control (DEC), (ii) drug free but with IVO24 and MF (IVO24-DEC-MF), (iii) containing PTX or DOXO but not IVO24 and without MF (DEC-PTX, DEC-DOXO), (iv) containing PTX or DOXO and with IVO24 but without MF (IVO24-DEC-PTX, IVO24-DEC-DOXO), (v) containing PTX and DOXO and with IVO 24 but without MF (IVO24-DEC-PD), (vi) containing PTX or DOXO and with IVO24 plus MF (IVO24-DEC-PTX-MF, IVO24-DEC-DOXO-MF), (vii) containing PTX and DOXO and with IVO 24 plus MF (IVO24-DEC-PD-MF). IVO24: targeting peptides; MF: high frequency magnetic field treatment for 2.5 min.

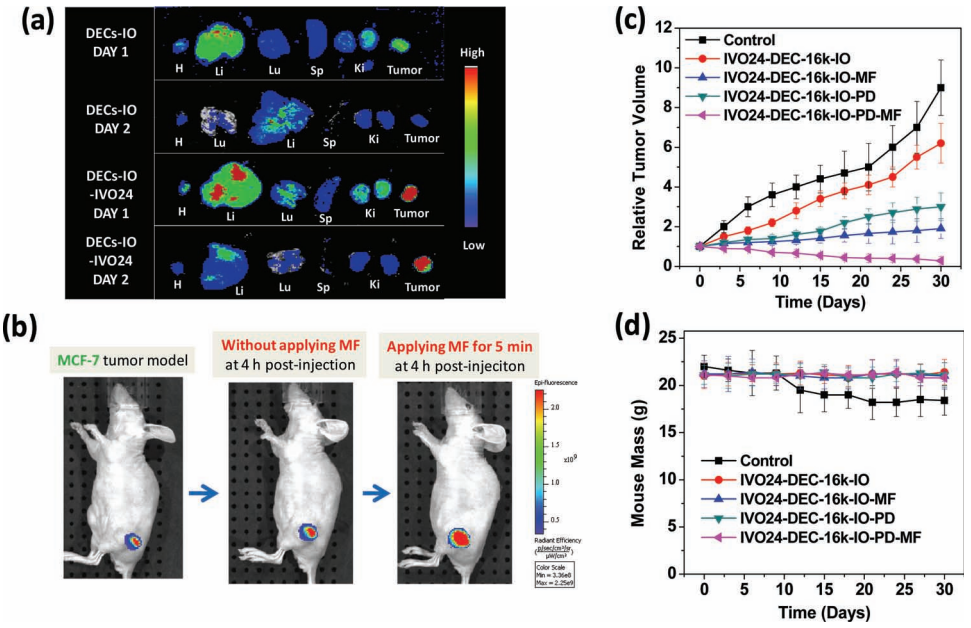

Figure 4. (a) Fluorescence images of organs from MCF-7 tumor bearing mice 24 h and 48 h after quantum-dot-labeled-capsule (DEC-16k-IO and IVO24-DEC-16k-IO) injection (i.v.). (b) In vivo drug (DOXO) release of DEC-16k-IO in solid tumor. Fluorescence signal (from DOXO, collected by IVIS imaging system) shown after injection directly into tumor, 4 h post injection, and after magnetic field treatment for 5 min subsequent to the 4 h post-injection examination. (c) Tumor therapy using DEC-16k-IO with/without drugs (PD = DOXO+PTX) and with/without magnetic field treatment (MF) for 10 min at 24 h post-injection. (d) Mouse mass as a function of days post-treatment showing no loss for 30 days in all groups.

notations used in Figure 3 and in the following discussion.) These are (i) control (DEC), (ii) drug free but with IVO24 and MF (IVO24-DEC-MF), (iii) containing PTX or DOXO but not IVO24 and without MF (DEC-PTX, DEC-DOXO), (iv) containing PTX or DOXO and with IVO24 but without MF (IVO24-DEC-PTX, IVO24-DEC-DOXO), (v) containing PTX and DOXO and with IVO 24 but without MF (IVO24-DEC-PD), (vi) containing PTX or DOXO and with IVO24 plus MF (IVO24-DEC-PTX-MF, IVO24-DEC-DOXO-MF), (vii) containing PTX and DOXO and with IVO 24 plus MF (IVO24-DEC-PD-MF). Several conclusions can be drawn from comparing these groups. First, MF alone can cause considerable cytotoxicity when the cells are targeted by IVO24-DEC-IO, reaching ~20% cell viability in group (ii). This is likely due to magneto-hyperthermia via magnetic induction of IO, which is internalized by the cells because of IVO24 targeting. Second, drug-containing but IVO24-free DECs are not very efficient, with cell viability in the 75% range (group (iii)). Third, the efficiency of drug-containing DEC is greatly enhanced by adding IVO24, lowering cell viability to 50% for DOXO and 35% for PTX (group (iv)); importantly, combining PTX and DOXO in the DEC lowers cell viability further to 10% (group (v)). Fourth, MF treatment of drug-containing, IVO24-guiding DEC is highly efficient, lowering cell viability to 10% when delivering DOXO, to 5% when delivering PTX (group (vi)), and to merely 2% when delivering both (group (vii)). These results completely confirm that, with the aid of cell targeting, the dual-drug, MF-trigger strategy made feasible by the PVA-16k-IO formulation is highly successful in vitro, with a major enhancement in the therapeutic efficacy realized every time when one additional element in the strategy (IVO24 targeting, dual drug, and MF trigger) is incorporated into the treatment protocol.

Consistent with the in vitro results, we found that targeting peptide IVO24 also improved the DEC-16k-IO accumulation in tumors in vivo. We injected quantum-dot-labeled DEC-16k-IO and IVO24-DEC-16k-IO through tail veins into nude mice bearing MCF-7 tumors to assess the biodistribution of DEC in major organs in addition to tumors. As shown in **Figure 4**a, IVO24-DEC-16k-IO is more efficiently accumulated in the tumor than DEC-16k-IO. While the latter showed some weak accumulation in the tumor 24 h post-injection, presumably because of tumor's enhanced permeability and retention (EPR) effects,[25,26] the fluorescence signal was washed out after 48 h indicating poor DEC-cell binding. In contrast, IVO-DEC-16k-IO showed very strong accumulation in the tumor at both 24 and 48 h, indicating that cell targeting when aided by possible internalization can result in persistent accumulation.

To implement magneto-chemotherapy, we injected 100 µL solution (saline solution with 2 wt% DEC) of IVO24-DEC-16k-IO-PD that contained both drugs into solid tumors of nude mice shown in Figure 4b. Fluorescence signal from DOXO (Ex: 535 nm, Em: 580 nm) was found to be initially localized to a small region around the point of injection (left panel), which spread out somewhat after 4 h (middle panel). Since DOXO originally resided in the core of DEC, its fluorescence signal was shielded by the surrounding IO-impregnated PVA shell, thus appeared weak. The mouse was next exposed to a 50 kHz MF (8 kA/m) for 5 min which caused a rapid expansion of the fluorescence-emitting region (right panel). This suggests that MF can trigger DOXO release from the core of DEC, and the released DOXO can subsequently migrate outward possibly with the aid of blood stream in the tumor vasculature.

To analyze the therapeutic effect, we compared tumor growth up to 30 days in mice receiving the following treatments: (i) control, (ii) IVO24-DEC-16k-IO injected, (iii) IVO24-DEC-16k-IO-PD injected, (iv) (ii) followed by MF treatment (50 kHz, 8 kA/m) for 10 min at 24 h post injection, and (v) (iii) followed by the same MF treatment. As shown in Figure 4c, only treatment (v) resulted in a reduction of the turmor size although treatment (iii) nearly arrested tumor growth whereas treatment (iv) arrested tumor growth for the first 15 days. These results confirmed the therapeutic effects of (a) the MF treatment (i.e., magneto-hyperthermia, mediated here by IO in the DEC, as evidenced by the drug-free treatment (iv)), and (b) the dual-drug PTX-DOXO (treatment (iii)), but it is the combined use of MF and dual-drug that is most effective. Meanwhile, judging from the absence of weight loss shown in Figure 4d, there appears to be little side effect/systematic toxicity of either magneto-hyperthermia or magneto-chemotherapy when administered with our highly engineered DEC-IO systems, with or without drugs.

In summary, (1) we have developeda one-step emulsifying method to fabricate core-shell W/O/W nanocapsules with a single-component-polymer PVA shell stabilized by iron oxide nanoparticles. This simple, versatile and scalable method was used to encapsulate hydrophilic DOXO and hydrophobic PTX with high efficiency. (2) We have achieved on-demand drug release in vitro and in vivo using a high frequency magnetic field trigger. The release profile displays features of fast on/off-acting and a precise field-dosage dependence, making it highly controllable. (3) We have demonstrated cell kill in vitro and tumor growth suppression in vivo by magneto-chemotherapy using drug-containing tumor-targeting nanocapsules, with little side effect. Magneto-hyperthermia using iron-oxide-containing tumor-targeting nanocapsules without chemotherapy drugs was also found effective for treating tumor. (4) We suggest the delivery platform developed here can facilitate various integrated theranostic protocols that combine multiple hydrophobic/hydrophilic drugs, target/remote-field sensing, on-demand drug release, hyperthermia, and MR imaging. Such multifunctional nano-platforms may open a new avenue for cancer treatment, possibly leading to clinical applications.

Experimental Section

Detail experimental procedures are described in Supporting Information.

Supporting Information

Supporting Information is available from the Wiley Online Library or from the author.

Acknowledgements

This work is financially supported by Magmedical Technologies Corporation and the National Science Council of the Republic of China, Taiwan under Contract of NSC 100-2320-B-009-006-MY2 and NSC 99-2221-E-009-070-MY3. This work is also supported by the "Aim for the Top University" program of the National Chiao Tung University and Ministry of Education, Taiwan, R.O.C. I.-W.C. acknowledges support from Army Medical Research & Material Command Grant No. W81XWH-10-1-0320 and W81XWH-10-1-0604. We are grateful to Dr. Chi-Sheng Hsiao for the carrier analysis and fruitful discussion.

Received: March 27, 2012
Revised: April 20, 2012
Published online: June 12, 2012

[1] Y. Wang, S. Gao, W. H. Ye, H. S. Yoon, Y. Y. Yang, *Nat. Mater.* **2006**, *5*, 791.
[2] C. E. Ashley, E. C. Carnes, G. K. Phillips, D. Padilla, P. N. Durfee, P. A. Brown, T. N. Hanna, J. Liu, B. Phillips, M. B. Carter, N. J. Carroll, X. Jiang, D. R. Dunphy, C. L. Willman, D. N. Petsev, D. G. Evans, A. N. Parikh, B. Chackerian, W. Wharton, D. S. Peabody, C. J. Brinker, *Nat. Mater.* **2011**, *10*, 389.
[3] X. B. Xiong, A. Lavasanifar, *ACS Nano* **2011**, *5*, 5202.
[4] H. Meng, M. Liong, T. Xia, Z. Li, Z. Ji, J. I. Zink, A. E. Nel, *ACS Nano* **2010**, *4*, 4539.
[5] H. Wang, P. Zhao, W. Su, S. Wang, Z. Liao, R. Niu, J. Chang, *Biomaterials* **2010**, *31*, 8741.
[6] W. Chen, F. Meng, R. Cheng, Z. Zhong, *J. Control. Release* **2010**, *142*, 40–46.
[7] P. D. Torre, A. R. Imondi, C. Bernardi, A. Podestà, D. Moneta, M. Riflettuto, G. Mazueé, *Cancer Chemother. Pharmacol.* **1999**, *44*, 138.
[8] T. Onda, N. Katsumata, R. Tsunematsu, T. Yasugi, M. Mushika, K. Yamamoto, T. Fujii, T. Hirakawa, T. Kamura, T. Saito, H. Yoshikawa, *Jpn. J. Clin. Oncol.* **2004**, *34*, 540.
[9] D. L. Gustafson, A. L. Merz, M. E. Long, *Cancer Lett.* **2005**, *220*, 161.
[10] B. J. Sun, H. C. Shum, C. Holtze, D. A. Weitz, *ACS Appl. Mater. Interfaces* **2010**, *2*, 3411.
[11] K. Landfester, *Angew. Chem. Int. Ed.* **2009**, *48*, 4488.
[12] S. H. Kim, H. C. Shum, J. W. Kim, J. C. Cho, D. A. Weitz, *J. Am. Chem. Soc.* **2011**, *133*, 15165.
[13] A. S. Utada, E. Lorenceau, D. R. Link, P. D. Kaplan, H. A. Stone, D. A. Weitz, *Science* **2005**, *308*, 537.
[14] J. A. Hanson, C. B. Chang, S. M. Graves, Z. Li, T. G. Mason, T. J. Deming, *Nature* **2008**, *455*, 85.
[15] Y. Wang, T. Zhang, G. Hu, *Langmuir* **2006**, *22*, 67.
[16] M. F. Ficheux, L. Bonakdar, F. Leal-Calderon, J. Bibette, *Langmuir* **1998**, *14*, 2702.
[17] C. Wasan, A. H. Ghassemi, W. E. Hennink, S. Okonogi, *Colloids Surf. B: Biointerfaces* **2011**, *84*, 508.
[18] X. Cheng, R. Liu, Y. He, *Eur. J. Pharm. Biopharm.* **2010**, *76*, 336.
[19] J. Yao, B. A. Tucker, X. Zhang, P. Checa-Casalengua, R. Herrero-Vanrell, M. J. Young, *Biomaterials* **2011**, *32*, 1041.
[20] S. U. Pickering, *J. Chem. Soc.* **1907**, *19*, 2001.
[21] B. P. Binks, T. S. Horozov, in *Colloidal Particles at Liquid Interfaces*, Cambridge University Press, Cambridge, **2006**.
[22] C. Miesch, I. Kosif, E. Lee, J. K. Kim, T. P. Russell, R. C. Hayward, T. Emrick, *Angew. Chem. Int. Ed.* **2012**, *51*, 145.
[23] T. Y. Liu, K. H. Liu, D. M. Liu, S. Y. Chen, I. W. Chen, *Adv. Funct. Mater.* **2009**, *19*, 616.
[24] T. Y. Liu, S. S. Hu, D. M. Liu, S. Y. Chen, I. W. Chen, *Nano Today* **2009**, *4*, 52.
[25] R. Duncan, *Nat. Rev. Drug Discov.* **2003**, *2*, 347.
[26] D. Peer, K. M. Karp, S. Hong, O. C. Farokhzad, R. Margalit, R. Langer, *Nature Nanotechnol.* **2007**, *2*, 751.